



1 **Distinct aerosol effects on cloud-to-ground lightning in the**
2 **plateau and basin regions of Sichuan, Southwest China**

3

4 Pengguo Zhao^{1,2,3}, Zhanqing Li², Hui Xiao⁴, Fang Wu⁵, Youtong Zheng²,
5 Maureen C. Cribb², Xiaoi Jin⁵, Yunjun Zhou¹

6

7 ¹Plateau Atmosphere and Environment Key Laboratory of Sichuan Province, College
8 of Atmospheric Science, Chengdu University of Information Technology, Chengdu
9 610225, China

10 ²Department of Atmospheric and Oceanic Science, Earth System Science
11 Interdisciplinary Center, University of Maryland, College Park, MD 20742, USA

12 ³Key Laboratory for Cloud Physics of China Meteorological Administration, Beijing
13 100081, China

14 ⁴Guangzhou Institute of Tropical and Marine Meteorology, China Meteorological
15 Administration, Guangzhou 510640, China

16 ⁵State Laboratory of Remote Sensing Sciences, College of Global Change and Earth
17 System Science, Beijing Normal University, Beijing 100875, China

18

19 Correspondence: Zhanqing Li (zhanqing@umd.edu) and Pengguo Zhao
20 (zpg@cuit.edu.cn)

21

22

23

24

25

26

27



28 **Abstract.** The joint effects of aerosol, thermodynamic, and cloud-related factors on
29 cloud-to-ground lightning in Sichuan were investigated by a comprehensive analysis of
30 ground measurements made from 2005 to 2017 in combination with reanalysis data.
31 Data include aerosol optical depth, cloud-to-ground (CG) lightning density, convective
32 available potential energy (CAPE), mid-level relative humidity, lower- to mid-
33 tropospheric vertical wind shear, cloud-base height, total column liquid water (TCLW),
34 and total column ice water (TCIW). Results show that CG lightning density and
35 aerosols are positively correlated in the plateau region and negatively correlated in the
36 basin region. Sulfate aerosols are found to be more strongly associated with lightning
37 than total aerosols, so this study focuses on the role of sulfate aerosols in lightning
38 activity. In the plateau region, the lower aerosol concentration stimulates lightning
39 activity through microphysical effects. Increasing the aerosol loading reduces the cloud
40 droplet size, reducing the cloud droplet collision-coalescence efficiency and inhibiting
41 the warm-rain process. More small cloud droplets are transported above the freezing
42 level to participate in the freezing process, forming more ice particles and releasing
43 more latent heat during the freezing process. Thus, an increase in aerosol loading
44 increases CAPE, TCLW, and TCIW, stimulating CG lightning in the plateau region. In
45 the basin region, by contrast, the higher concentration of aerosols inhibits lightning
46 activity through the radiative effect. An increase in aerosol loading reduces the amount
47 of solar radiation reaching the ground, thereby lowering CAPE. The intensity of
48 convection decreases, resulting in less supercooled water transported to the freezing
49 level and fewer ice particles forming, thus increasing the total liquid water content.
50 Therefore, an increase in aerosol loading suppresses the intensity of convective activity
51 and CG lightning in the basin region.

52

53

54

55

56



57 **1 Introduction**

58

59 Aerosol-cloud-precipitation interactions are complicated, mainly reflected in the
60 influence of aerosols on cloud microphysical and radiation processes, i.e., aerosol-cloud
61 interactions (ACI) and aerosol-radiation interactions (ARI) (Rosenfeld et al., 2008;
62 Huang et al., 2009; Koren et al., 2014; Li et al., 2011, 2017, 2019; Oreopoulos et al.,
63 2020). The aerosol microphysical effect refers to the role of aerosols as cloud
64 condensation nuclei (CCN) and ice nuclei (IN), influencing the microphysical
65 processes of liquid- and ice-phase clouds. The aerosol radiation effect refers to the
66 absorption and scattering of solar radiation by aerosols, changing the radiation balance
67 between the atmosphere and the surface. The microphysical and radiative effects of
68 aerosols combined with dynamic processes influence weather and climate processes
69 through their links with meteorological conditions.

70 Lightning activity is mainly affected by atmospheric thermodynamic conditions
71 and is an important indicator of the development of convective systems. The collision
72 and separation of large and small ice particles mainly cause electrification. Supercooled
73 water, ice particles, and strong updrafts are the components needed for the occurrence
74 and development of lightning (MacGorman et al., 2001; Mansell et al., 2005; Williams,
75 2005; Price, 2013; Q. Wang et al., 2018; Qie and Zhang, 2019).

76 The differences in thermal conditions and aerosol loading between land and ocean
77 areas lead to a higher lightning frequency over land than over oceans (Williams and
78 Stanfill, 2002; Williams et al., 2004). Lightning activity over cities with higher aerosol
79 concentrations are more intense than that over clean suburbs (Westcott, 1995; Pinto et
80 al., 2004; Kar et al., 2009; Kar and Liou, 2014; Proestakis et al., 2016; Yair, 2018;
81 Tinmaker et al., 2019). An increase in aerosol concentration leads to the formation of
82 more small cloud droplets, which have difficulty forming raindrops due to their low
83 collision-coalescence efficiency, thus inhibiting the warm-rain process. These small
84 cloud droplets are transported above the freezing level, increasing the supercooled
85 water content in a thunderstorm and significantly enhancing the ice-phase process. The



86 freezing process releases more latent heat to stimulate convection, allowing more ice
87 particles to participate in the electrification process of collision and separation, thus
88 enhancing lightning activity (Khain et al., 2008; Mansell and Ziegler, 2013; P. Zhao et
89 al., 2015; Shi et al., 2015). A similar enhancement in lightning activity due to aerosols
90 was also found in oceanic regions, where aerosols and their precursors discharged by
91 ships significantly enhanced lightning activity over ship lanes (Thornton et al., 2017).
92 The influence of aerosols on thunderstorms is not linear. When the aerosol optical depth
93 (AOD) is less than 0.3, aerosols can stimulate lightning activity. However, the intensity
94 of lightning activity will be inhibited if the concentration of aerosols increases (Altartz
95 et al., 2010; Stallins et al., 2013; X. Li et al., 2018; Q. Wang et al., 2018).

96 The effect of aerosols on convective clouds and lightning activity is not only
97 controlled by environmental factors, but also by aerosol type. Absorbing aerosols block
98 solar radiation from reaching the surface through radiative effects, which tends to
99 inhibit the development of convection. Hygroscopic aerosols can stimulate the
100 development of thunderstorms through microphysical effects under appropriate
101 environmental conditions (Wang et al., 2018). In central China, aerosol absorption of
102 solar radiation has increased the stability of the lower atmosphere, reducing
103 thunderstorm activity by 50% from 1961 to 2000 (Yang et al., 2013). In Nanjing in
104 eastern China, aerosols reduced the amount of solar radiation reaching the surface and
105 the convective available potential energy (CAPE), inhibiting the intensity of lightning
106 activity (Tan et al., 2016). In the Sichuan Basin, with its complex topography, the
107 influence of absorbing aerosols on strong convection is more complicated. During the
108 day, aerosols absorb solar radiation and increase the stability of the lower atmosphere,
109 accumulating a large amount of water vapor and energy in the basin. Under the
110 influence of the uplift of the mountain terrain at night, convection is excited, and
111 stronger convective precipitation is formed in the mountainous area (Fan et al., 2015).
112 In southeast China where the hygroscopicity of aerosols dominates, an increase in
113 aerosols in the plain areas significantly stimulates lightning activity (Yuan et al., 2011;
114 Y. Wang et al., 2011), while the influence of aerosols on thunderstorms in mountainous



115 areas with slightly higher altitudes is not prominent (Yang and Li, 2014). Aerosol
116 radiative and microphysical effects have different impacts on thunderstorms at different
117 stages of their development. In the Pearl River Delta region, the daytime radiative effect
118 delays lightning activity, while the aerosol microphysical effect at night further
119 stimulates lightning activity (Guo et al., 2016; Lee et al., 2016).

120 The eastern part of Sichuan province is a large basin, and the western part is the
121 easternmost part of the Tibetan Plateau. The thermal and moisture conditions in the
122 basin facilitate lightning activity (Xia et al., 2015; Yang et al., 2015). The Sichuan basin
123 is an area with high aerosol loading and with terrain not conducive to pollutant diffusion
124 (X. Zhang et al., 2012; L. Sun et al., 2016; Wei et al., 2019a, b). In this study, we
125 investigate the joint effects of aerosol, thermodynamic, and cloud-related conditions on
126 cloud-to-ground (CG) lightning activity under such special topographic conditions.

127 We mainly focus on the influence of aerosol, thermodynamic, and microphysical
128 factors on CG lightning density. Previous studies have suggested that aerosols affect
129 the intensity and polarity of lightning (Lyons et al., 1998; Naccarato et al., 2003; Carey
130 et al., 2007; Pawar et al., 2017). Future studies involving observational data analyses
131 and numerical simulations will investigate the mechanism by which aerosols affect the
132 lightning polarity by modulating the charge structure. This paper is organized as follows.
133 Section 2 describes the data and methodology used in the study. Section 3 presents and
134 discusses the results, and section 4 summarizes the study.

135

136 **2 Data and methodology**

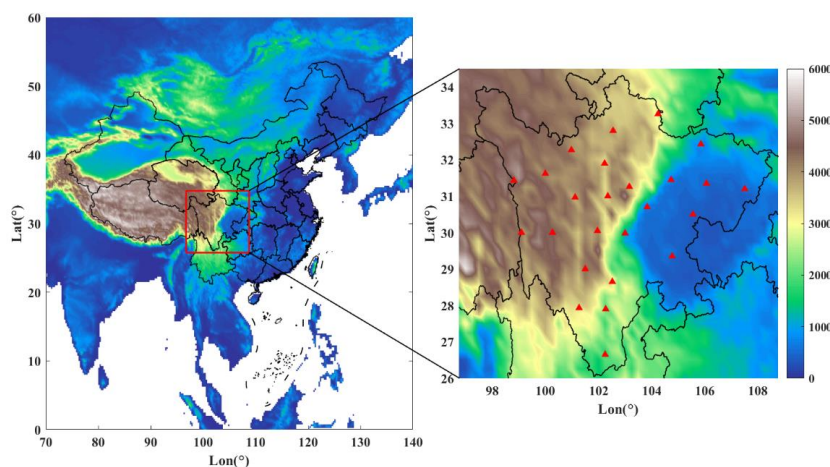
137 **2.1 CG lightning**

138 Sichuan province is in southwest China, with the Qinghai-Tibet Plateau and
139 Hengduan Mountains to the west, the Qinba Mountains to the north, and the Yunnan-
140 Guizhou Plateau to the south (Fig. 1). The western part of Sichuan province is
141 dominated by plateau and mountainous terrain, with an average elevation of about 2000
142 to 4000 m, while the eastern part is dominated by a basin and hilly terrain, with an
143 average elevation of 300 to 700 m.



144 Hourly CG lightning flashes data from 2005 to 2017 were obtained from the
145 Sichuan Meteorological Bureau. CG lightning flashes are observed by the Sichuan
146 Lightning Detection Network (SLDN), which belongs to the China Lightning Detection
147 Network of the China Meteorological Administration (CMA), and consists of 25
148 detection sensors (Fig. 1). The average detection accuracy of the sensor is ~300 m, the
149 average detection radius is 300 km, and the detection efficiency is 80–90% (Yang et al.,
150 2015). The SLDN is based on the ground-based Advanced Time of Arrival and
151 Direction system, which uses improved accuracy from the combined technology
152 method (Cummins et al., 1998; CMA, 2009).

153 Positive CG lightning flashes with peak currents less than 15 kA are removed to
154 avoid the contamination of cloud-to-cloud lightning (Cummins and Murphy, 2006). A
155 flash is identified if the location of the first stroke is within 10 km, and the time interval
156 between two contiguous strokes is less than 0.5 seconds. If the polarity of the stroke is
157 different, it is a different flash (Cummins et al., 1998). To match the thermodynamic
158 and cloud-related parameters, the CG lightning data used in this study were calculated
159 at a 0.25° horizontal resolution. Many previous studies (e.g., Orville et al., 2011; Ramos
160 et al., 2011; Yang et al., 2015) have also discussed the basic characteristics of lightning
161 at a similar resolution.



162
163 **Figure 1.** Location of Sichuan province with the color-shaded background showing



164 terrain heights (unit: m). The zoomed image shows the locations of the lightning sensors
165 (red triangles).

166

167 **2.2 AOD**

168 The Modern-Era Retrospective analysis for Research and Applications, version 2
169 (MERRA-2), dataset provided AODs from 2005 to 2017. The quality-controlled
170 MERRA-2 AOD product (at 550 nm) provides the optical thicknesses of different types
171 of aerosols, including total aerosol, sulfate, black carbon, organic carbon, and dust, with
172 a spatial resolution of $0.5^{\circ} \times 0.625^{\circ}$ (Randles et al., 2017; Buchard et al., 2017). To
173 match CG lightning data, we interpolated AOD data onto the same 0.25° spatial
174 resolution grid. The horizontal distribution and vertical structure of MERRA-2 aerosol
175 optical properties are in good agreement with satellite and aircraft observations
176 (Buchard et al., 2017). E. Sun et al. (2018, 2019) employed MODerate resolution
177 Imaging Spectroradiometer (MODIS) and Aerosol Robotic Network (AERONET)
178 AOD products to evaluate the MERRA-2 AOD over China. They reported that the
179 MERRA-2 and MODIS AODs agreed well and that the seasonal correlation coefficients
180 between the MERRA-2 and AERONET AODs ranged from 0.87 to 0.92.

181 **2.3 Thermodynamic and cloud-related parameters**

182 Thermodynamic and cloud-related factors include CAPE, mid-level relative
183 humidity (RH), lower- to mid-tropospheric vertical wind shear (SHEAR), cloud-base
184 height (CBH), total column liquid water (TCLW), and total column ice water (TCIW),
185 collected from ERA5 reanalysis data with a spatial resolution of $0.25^{\circ} \times 0.25^{\circ}$ (Dee et
186 al., 2011).

187 Hoffmann et al. (2019) indicated that the ERA5 reanalysis is more representative
188 of atmospheric convection, mesoscale cyclones, and mesoscale to synoptic-scale
189 atmospheric characteristics than the earlier ERA-Interim reanalysis. Freychet et al.
190 (2020) found that the dry-bulb temperature, wet-bulb temperature, and RH of the ERA5
191 reanalysis were representative through comparisons with ground observations made in
192 China. S. Lee et al. (2018) compared the water vapor and liquid water distributions
193 observed by a microwave radiometer in Seoul, South Korea, with that of the ERA5



194 reanalysis and found that they agreed well. Shou et al. (2019) confirmed that ERA5
195 data captured the cloud-top features based on multi-satellite observations made over the
196 Tibetan Plateau. Zhang et al. (2019) pointed out that the ERA5 precipitable water vapor
197 field agreed well with radiosonde and Global Navigation Satellite System observations.
198 Lei et al. (2020) examined the representation of ERA5 cloud-cover characteristics over
199 China through comparisons with satellite observations, reporting that (1) ERA5
200 overestimated the cloud cover by ~10%, and (2) the long-term trend in ERA5 cloud
201 cover was consistent with satellite observations. These studies suggest that ERA5
202 cloud-related data from China have sound quality.

203 CAPE is the most important factor controlling lightning, and climate projections
204 suggest that an increase in CAPE caused by global warming could increase global
205 lightning by 50% in the twenty-first century (Romps et al., 2014). The proxy composed
206 of precipitation rate and CAPE has a good correlation with observed lightning density
207 over the United States (Romps et al., 2018; Tippett and Koshak, 2018; Tippett et al.,
208 2019). CAPE is the factor with the highest relative contribution in various lightning
209 parameterization schemes (Bang and Zipser, 2016; Stolz et al., 2015, 2017).

210 Due to the large elevation fluctuation in Sichuan, pressure-level data are not
211 applicable to the analysis of the atmospheric vertical structure. So, pressure levels were
212 changed to geometric altitudes above ground level (AGL), using the barometric formula
213 (Minzner, 1977)

$$214 \quad Z_2 = Z_1 + 18410 \left(1 + \frac{t_a}{273.15} \right) \log \frac{P_1}{P_2}, \quad (1)$$

215 where Z_2 and Z_1 are the elevations of the two isobaric levels (in m), P_2 and P_1 are the
216 pressures of the two isobaric levels (in hPa), P_1 is 1000 hPa, Z_1 is 0 m, and t_a is the
217 average temperature of the two isobaric levels (in °C). The elevation minus topographic
218 height is the altitude AGL,

$$219 \quad H = Z_2 - H_t, \quad (2)$$

220 where H is the geometric altitude AGL, and H_t is the topographic height.

221 The mid-level RH and the lower- to mid-tropospheric SHEAR are important
222 humidity and dynamic parameters, directly affecting the formation, development,



223 propagation, and intensity of thunderstorms (Davies-Jones, 2002; Thompson et al.,
224 2007; Wall et al., 2014; Bang and Zipser, 2016). In this study, RH is the average RH in
225 the 3–5-km layer, and SHEAR is the vertical wind shear in the 0–5-km layer:

$$226 \quad \text{SHEAR} = \sqrt{(u_2 - u_1)^2 + (v_2 - v_1)^2}, \quad (3)$$

227 where u_2 , u_1 , v_2 , and v_1 are zonal and meridional wind speeds at 5 km and 3 km,
228 respectively.

229 CBH, TCLW, and TCIW were selected to represent cloud-related parameters
230 affecting the development of lightning activity. CBH, negatively correlated with the
231 warm-cloud thickness, controls the convective structure and the polarity and intensity
232 of CG lightning by affecting the liquid water and ice water contents (Williams et al.,
233 2005; Carey and Buffalo, 2007; Stolz et al., 2017). Liquid water and ice water,
234 especially in the non-inductive electrification zone, directly control the processes of
235 charge generation and separation that determines the intensity of lightning of a
236 thunderstorm (Yair et al., 2010; Wong et al., 2013; Dafis et al., 2018).

237 In this study, we use Pearson correlation and partial correlation to discuss the
238 relationship between two elements at each grid point. Data from 156 months during the
239 period 2005–2017 were used, and monthly averages were calculated. Data at each grid
240 point were processed using a three-point moving average.

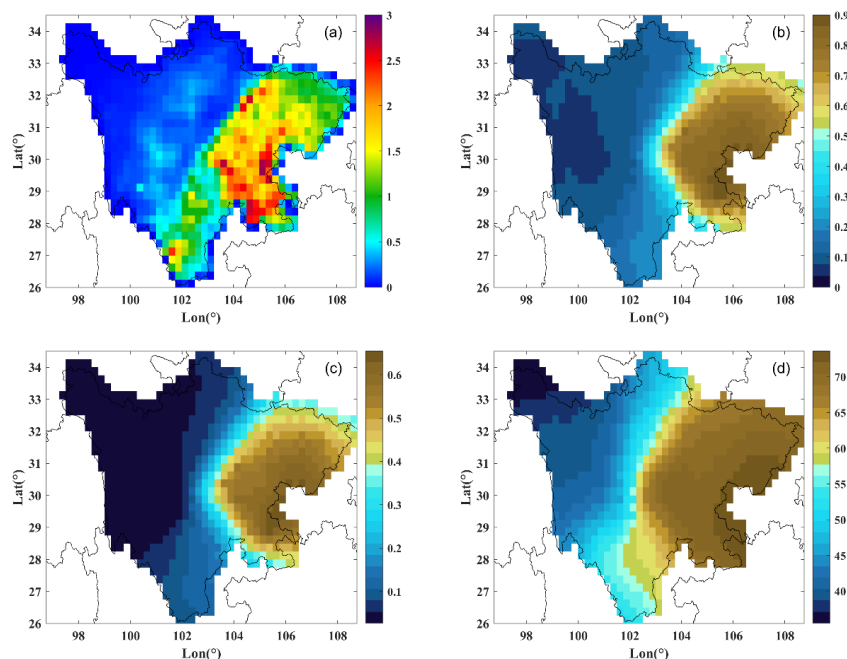
241 **3 Results and discussion**

242 **3.1 Distributions of CG lightning and AOD**

243 Due to the complex terrain in Sichuan, the CG lightning density and AOD differ
244 greatly across the province. The CG lightning density is highest over the basin region
245 in eastern Sichuan, with an annual average density of 1–3 flashes $\text{km}^{-2} \text{yr}^{-1}$ (Fig. 2a).
246 The lightning density in western Sichuan is much lower than that in the basin region.
247 Yang et al. (2015) showed that the Sichuan basin is one of the most CG-lightning-active
248 regions in China, besides the Yangtze River Delta and the Pearl River Delta. The
249 dramatic difference in lightning density between the basin and the plateau stems
250 primarily from differences in humidity and thermal conditions. Another factor is the
251 generation of strong convective systems caused by the eastward migration of the



252 southwest vortex formed over the Tibetan Plateau to the basin area (Yu et al., 2007;
253 Zhang et al., 2014). The total AOD over the basin region is significantly higher than
254 that over the plateau region. The mean AOD over the basin is about 0.6–0.9, while that
255 over the plateau is about 0.15 (Fig. 2b). The aerosols in Sichuan are mainly composed
256 of sulfate aerosols, accounting for about 60–80% of the total AOD over the basin and
257 40–55% of the total AOD over the plateau (Fig. 2d). Aerosol concentrations over the
258 basin are higher than those over the plateau area, mainly because of the greater amount
259 of anthropogenic air pollutants emitted in the basin (Zhang et al., 2012). Also playing
260 important roles are the mountains around the basin and the low-pressure system at 700
261 hPa over the basin, resulting in a strong inversion above the planetary boundary layer
262 (Ning et al., 2018).



263 **Figure 2.** Distribution of (a) CG lightning density (unit: flashes $\text{km}^{-2} \text{yr}^{-1}$), (b) total
264 AOD, (c) sulfate AOD, and (d) percentage of sulfate AOD in total AOD (unit: %) over
265 Sichuan.

266

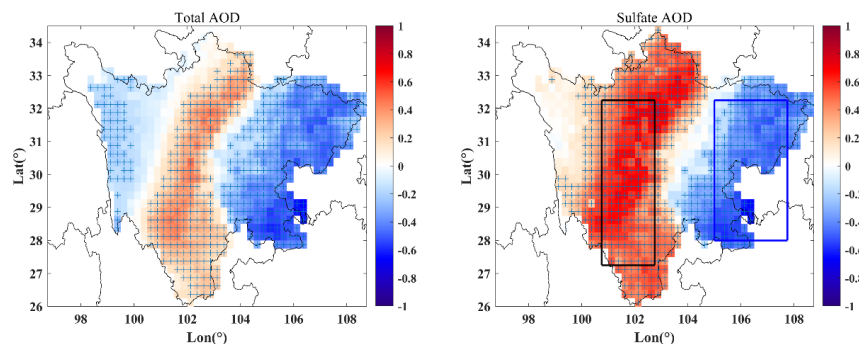
267 3.2 Correlation between AOD and CG lightning

268 While the spatial patterns of lightning intensity (Fig. 2a) and AOD (Fig. 2b) bear



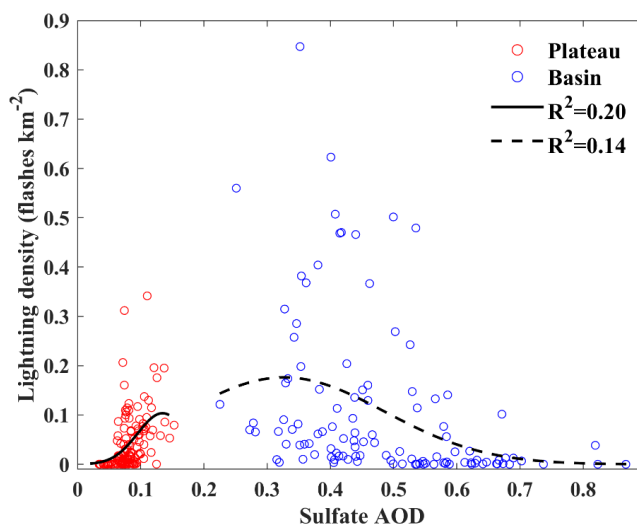
269 some resemblance, one cannot draw a straight conclusion that the latter is the cause of
270 the former because they are both influenced by the topography. However, the influences
271 of aerosols on lightning have been well established in previous studies by affecting the
272 local meteorological environment through aerosol radiative and microphysical effects
273 (Yang et al., 2013; Q. Wang et al., 2018; Z. Li et al., 2019). To circumvent the
274 topographic influence, Fig. 3 shows the Pearson correlation coefficients of total
275 AOD/sulfate AOD and CG lightning density in individual grid boxes in Sichuan. It is
276 interesting to note that the correlation between aerosol loading and lightning is opposite
277 in the plateau region and the basin region, i.e., a positive correlation in the plateau
278 region and a negative correlation in the basin region. This suggests that aerosols
279 stimulate lightning in the plateau region, but suppress lightning in the basin region.
280 Such a distinct difference may be related to differences in aerosol loading and local
281 environmental factors (Rosenfeld et al., 2007; Fan et al., 2009; Carrió and Cotton, 2014).
282 The maximum value of the positive correlation coefficient was about 0.5, occurring in
283 the plateau region of central Sichuan. The maximum values of the negative correlation
284 coefficients occurred in the basin region of eastern Sichuan. The absolute values of the
285 negative correlation coefficients are larger than those of the positive correlation
286 coefficients. The distribution of the correlation coefficients between lightning and
287 sulfate AOD is similar to that of total AOD, but there are more and larger positive
288 correlation coefficients than negative ones. Since sulfate AOD accounts for more than
289 80% of the total AOD in Sichuan, this study mainly discusses the relationship between
290 sulfate AOD and lightning activity.

291 Note that a statistical relationship between two variables does not necessarily
292 imply a true causality between the two for which much further insights are needed. The
293 spatial contrast exhibited in the correlation maps, however, conveys valuable
294 information about the causality because the influences of large-scale meteorology may
295 have little to do with the spatial pattern. The plateau and basin regions in this study are
296 outlined in Fig. 3 (right panel) to discuss the effects of sulfate aerosols on lightning
297 activity in the two regions separately.



298 **Figure 3.** Pearson correlation coefficients between total AOD and CG lightning (left
299 panel) and sulfate AOD and CG lightning (right panel) based on monthly data from
300 2005 to 2017. The correlation coefficient of each grid box is calculated from 156
301 monthly average datasets, and monthly average data are processed using a three-point
302 moving average. Crosses in the figure indicate grid boxes that have passed the 95%
303 significance test. The plateau region and the basin region are outlined by black and blue
304 rectangles, respectively, in the right panel.
305

306 To further analyze the relationship between aerosols and lightning over Sichuan,
307 Fig. 4 shows the CG lightning density as a function of sulfate AOD over the plateau
308 and basin regions. Due to differences in emissions, the aerosol loading over the plateau
309 region is much lighter than that over the basin region. The regional average sulfate AOD
310 over the plateau region ranges from 0.03 to 0.15, and that over the basin region ranges
311 from 0.22 to 0.87. The difference in CG lightning density is mainly related to the
312 different meteorological conditions of the plateau and the basin. The monthly regional
313 average CG lightning density over the plateau is 0.1×10^{-3} to 0.35 flashes km^{-2} , while
314 that over the basin is 0.1×10^{-3} to 0.85 flashes km^{-2} . In the plateau region, the lightning
315 density increases exponentially with increasing AOD, while in the basin region, the
316 lightning density decreases exponentially with increasing AOD. This difference may be
317 due to the different microphysical and radiative effects of different aerosol loadings.
318 Previous studies (Koren et al., 2008, 2012; Altaratz et al., 2010, 2017) have noted a
319 turning point of $\text{AOD} = 0.3$ with regard to the influence of AOD on clouds. For lower
320 AOD, aerosols can stimulate lightning activity through microphysical effects. For
321 higher AOD, aerosols reduce the solar radiation reaching the surface through the
322 radiative effect, thus inhibiting lightning activity.



323

324 **Figure 4.** CG lightning density as a function of sulfate AOD over the basin (blue circles)
325 and plateau (red circles) regions. Exponential-fit curves are shown, and coefficients of
326 determination (R^2) are given.

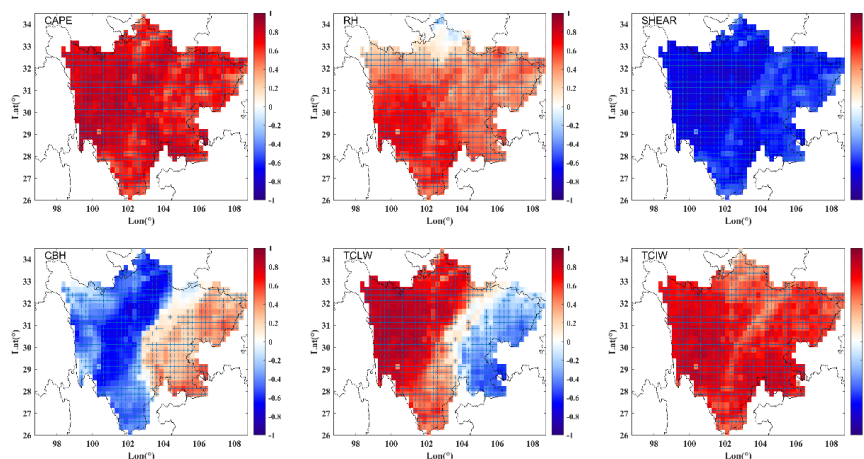
327

328 **3.3 Correlation between thermodynamic and cloud-related factors and CG** 329 **lightning**

330 Compared with the effect of aerosols on lightning activity, thermodynamic and
331 cloud-related parameters are the decisive factors determining the occurrence and
332 development of lightning activity (Williams, 2005; Williams et al., 2005; Saunders,
333 2008; Stolz et al., 2017). Figure 5 shows correlation coefficients between CAPE, RH,
334 SHEAR, CBH, TCLW, and TCIW, and CG lightning density over Sichuan. The
335 thermodynamic parameters CAPE and RH, especially CAPE, have significant
336 excitation effects on lightning activity, while SHEAR shows a significant negative
337 correlation with lightning. There is a positive correlation between TCIW and lightning
338 density over Sichuan because the development of lightning mainly depends on the non-
339 inductive electrification of the collision and separation of large and small ice particles.
340 The more ice particles, the stronger the lightning activity will be. The correlation
341 between CBH and lightning is opposite to that between TCLW and lightning in the
342 plateau and basin regions. Over the plateau area, low cloud bases and high liquid water



343 contents are favorable for lightning activity, while over the basin, the opposite is seen.
344 A higher CBH means that the warm-cloud depth is thinner, so the liquid water content
345 will be less. In the plateau region, because of the compression effect of the plateau
346 topography on clouds, the warm-cloud depth is much thinner than that in the basin
347 region. Increasing a fixed amount of liquid water is conducive to transporting
348 supercooled water to the upper layer and promoting the development of the ice-phase
349 process. The more vigorous the ice-phase process is, the more intense the lightning
350 activity will be. Over the basin, where warm clouds are thicker, an increase in liquid
351 water will more likely promote the development of the warm-rain process rather than
352 the ice-phase process.



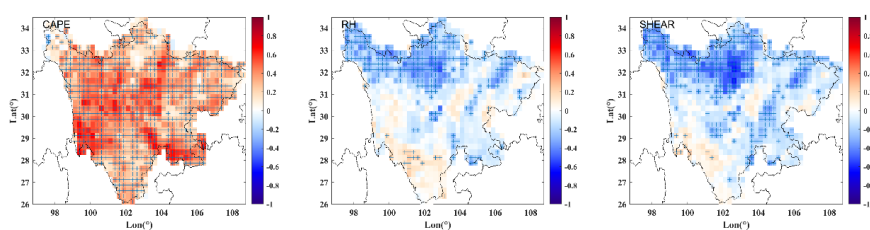
353 **Figure 5.** Pearson correlation coefficients between CAPE, RH, SHEAR, CBH, TCLW,
354 and TCIW and CG lightning. Crosses in the figure indicate grid boxes that have passed
355 the 95% significance test.

356

357 To avoid interactions between the factors involved and to discuss the relationships
358 between different factors and lightning activity more independently, Figs. 6 and 7,
359 respectively, show the partial correlation coefficients between thermodynamic and
360 cloud-related parameters and CG lightning density. In terms of the thermodynamic
361 parameters, the partial correlation coefficients show that the dependence of lightning
362 on RH and SHEAR is not significant. The partial correlation coefficient of some regions
363 in Sichuan is 0. Compared with RH, the absolute value of the negative partial



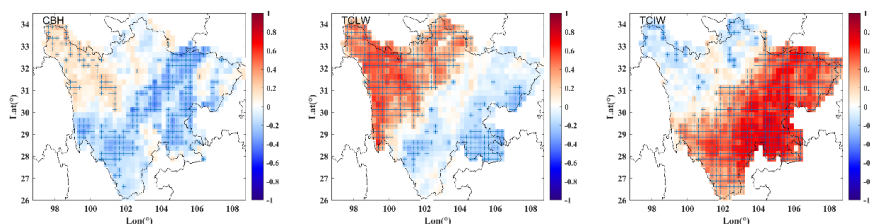
364 correlation coefficient of SHEAR is larger and more widely distributed, indicating that
365 SHEAR has a more significant impact (inhibition) on lightning activity than does RH.
366 CAPE is positively correlated with lightning in Sichuan, and the partial correlation
367 coefficient of many grid points is greater than 0.4, indicating that CAPE is a crucial
368 factor controlling lightning, as reported by others (Carey and Buffalo, 2007; Fuchs et
369 al., 2015; Bang and Zipser, 2016; Stolz et al., 2017).



370 **Figure 6.** Partial correlation coefficients between CG lightning and thermodynamic
371 factors, i.e., CAPE, RH, and SHEAR. Crosses in the figure indicate grid boxes that have
372 passed the 95% significance test.

373

374 Among the cloud-related parameters, the partial correlation coefficients between
375 CBH and TCLW and lightning are lower, indicating that CBH and TCLW have less
376 significant influences on lightning density (Fig. 7). The existence of supercooled water
377 is one of the essential conditions for the electrification of thunderstorms. The
378 supercooled liquid water content in different temperature ranges can affect the polarity
379 of the charge carried by ice particles but cannot directly affect the intensity of the
380 electrical activity of thunderstorms (Saunders et al., 1991; Saunders, 2008). The
381 positive partial correlation coefficient between TCLW and lightning is relatively higher,
382 especially in the basin area, indicating that ice particles, as the carrier of charge, can
383 directly determine the occurrence and development process of lightning activity.



384 **Figure 7.** Partial correlation coefficients between CG lightning and cloud-related
385 factors, i.e., CBH, TCLW, and TCIW. Crosses in the figure indicate grid boxes that have

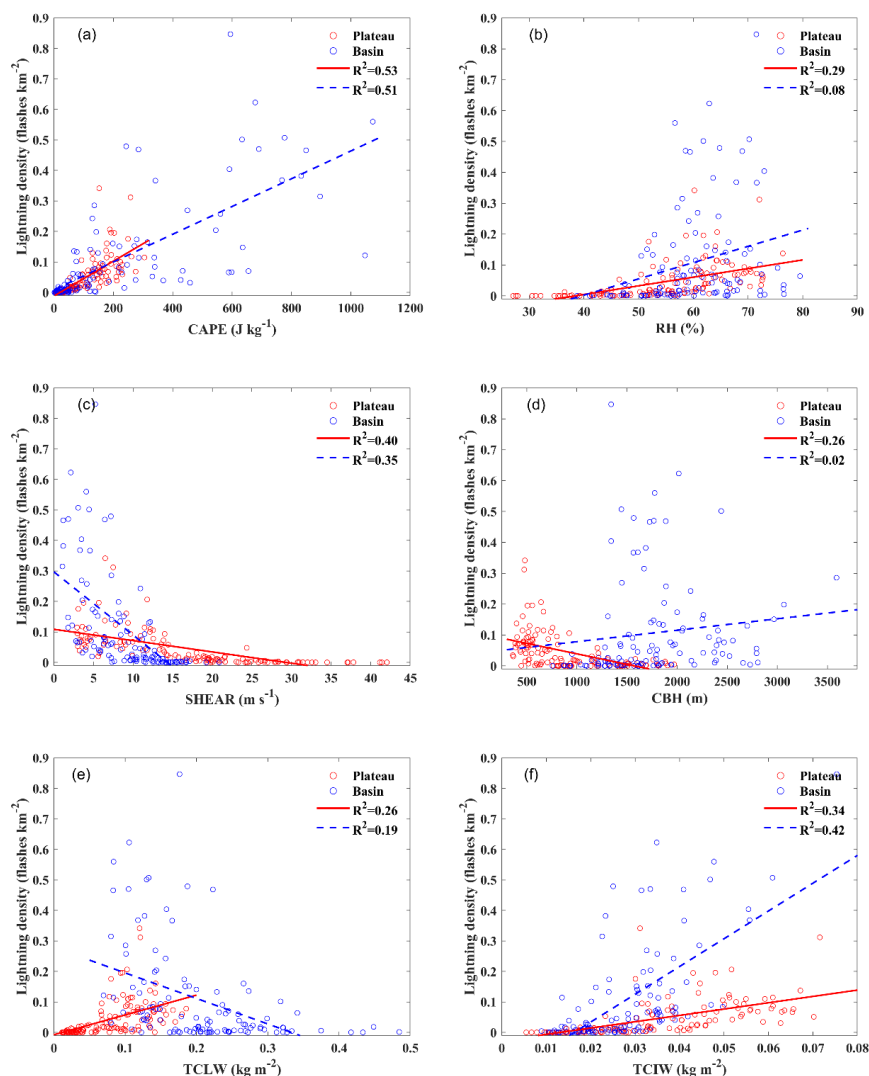


386 passed the 95% significance test.

387

388 To demonstrate the differences in thermodynamic and cloud-related factors
389 between the plateau and basin regions, Fig. 8 shows CG lightning density as a function
390 of the thermodynamic and cloud-related parameters in the plateau and basin regions,
391 based on monthly regionally averaged data. There is a significant positive correlation
392 between CAPE and CG lightning density in both the plateau and basin regions, with a
393 coefficient of determination (R^2) of 0.53 and 0.51, respectively. CAPE over the plateau
394 region is much smaller than that over the basin region. The maximum CAPE over the
395 plateau area is $\sim 300 \text{ J kg}^{-1}$, while the maximum CAPE over the basin area is over 1000
396 J kg^{-1} . This is the main reason why the CG lightning density over the basin region is
397 larger than that over the plateau region. RH and CG lightning density were positively
398 correlated in both plateau and basin regions, but not significantly in the basin region
399 ($R^2 = 0.08$). Due to the high altitude of the plateau and strong wind speeds there,
400 SHEAR in the plateau region (maximum value of 40 m s^{-1}) is significantly larger than
401 that in the basin region (maximum value of 15 m s^{-1}). The greater mid-level wind shear
402 over the plateau region suppresses the intensity of lightning activity.

403 Due to the compression of clouds by the plateau topography, the mean CBH over
404 the plateau region is relatively low, about 500–2000 m, while the mean CBH over the
405 basin region is about 1000–3500 m. The correlation between CBH and lightning density
406 is negative in the plateau. In the basin, however, there is barely any correlation ($R^2 =$
407 0.02). The much lower temperature over the plateau directly results in a lower liquid
408 water content there. The maximum value of TCLW is $\sim 0.2 \text{ kg m}^{-2}$, while that in the
409 basin region is $\sim 0.5 \text{ kg m}^{-2}$. Correlations in the plateau region are more significant than
410 in the basin region, with an R^2 of 0.26 and 0.19, respectively. The TCIWs over the
411 plateau and basin areas are similar in magnitude. The positive correlation between
412 TCIW and lightning density is also significant, with an R^2 of 0.34 and 0.42, respectively,
413 in the basin and plateau regions. Except for the correlation between CBH and lightning
414 in the basin region, the linear correlations between the other factors and lightning
415 passed the 95% significance test.



416 **Figure 8.** Lightning density as a function of thermodynamic and cloud-related factors
417 in the basin (blue circles) and plateau (red circles) regions: (a) CAPE, (b) RH, (c)
418 SHEAR, (d) CBH, (e) TCLW, and (f) TCIW. Linear-fit lines are shown, and coefficients
419 of determination (R^2) are given.

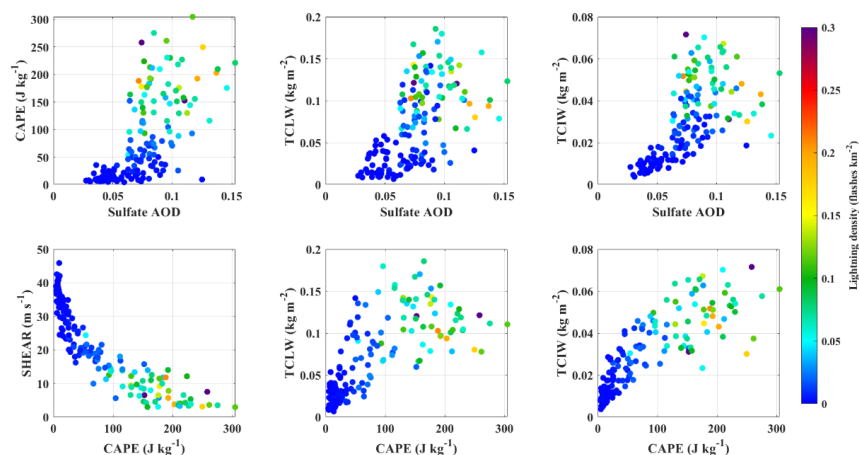
420

421 **3.4 Joint effects of thermodynamic and cloud-related factors and aerosols on CG** 422 **lightning**

423 Based on the partial correlation and linear fitting analyses, CAPE, SHEAR, TCLW,
424 and TCIW are the main thermodynamic and cloud-related factors controlling CG



425 lightning over the Sichuan region. To analyze the joint effects of thermodynamic factors,
426 Figs. 9 and 10 show scatter plots between sulfate AOD, CAPE, SHEAR, TCLW, and
427 TCIW, and CG lightning in the plateau and basin regions. In the plateau region (Fig. 9),
428 increases in CAPE, TCLW, and TCIW enhance lightning activity. As discussed before
429 (Fig. 8), strong convective activity and more liquid water and ice water indicate that
430 strong updrafts transport a greater amount of liquid-phase and ice-phase particles to the
431 electrification area to participate in the electrification process, generating stronger
432 lightning activity. Aerosol excitation of lightning may be achieved by increasing CAPE,
433 TCLW, and TCIW. In the case of low aerosol loading, through ACI, an increase in
434 aerosols will reduce the size of cloud droplets and increase the concentration of cloud
435 droplets (Khain et al., 2008; Qian et al., 2009). Smaller cloud droplets reduce the
436 collision-coalescence efficiency and inhibit the warm-rain process. Small cloud
437 droplets that do not fall are transported above the freezing layer to participate in the
438 freezing process and release more latent heat. This is consistent with previous studies
439 (Mansell et al., 2013; P. Zhao et al., 2015; Altaratz et al., 2017; Fan et al., 2018; C. Zhao
440 et al., 2018) and explains the potential cause of the increase in aerosols, leading to an
441 increase in liquid water and ice water in thunderstorms, promoting convective activities.
442 From the joint influence of CAPE, SHEAR, TCLW, and TCIW on lightning activity
443 (bottom panels of Fig. 9), an increase in CAPE inhibits the vertical wind shear in the
444 lower to middle troposphere, which is conducive to the development of lightning
445 activity. Increasing CAPE also suggests that strong updrafts promote the development
446 of convection, resulting in the formation of more liquid water and ice water in the cloud.



447

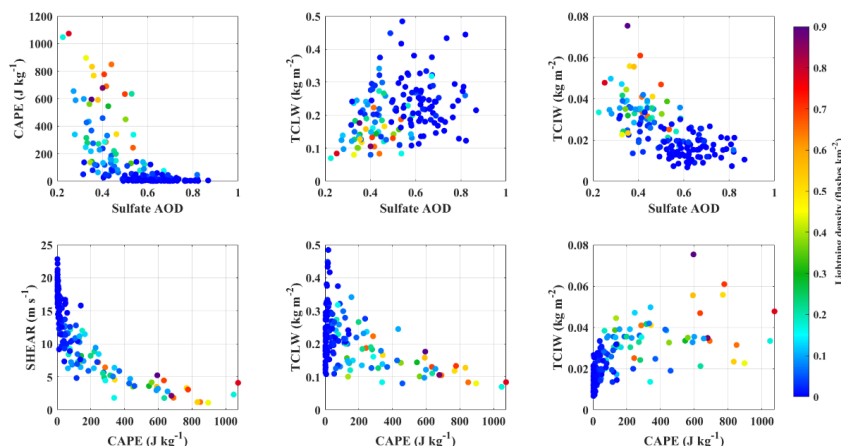
448 **Figure 9.** Joint effects of sulfate AOD, CAPE, SHEAR, TCLW, and TCIW on CG
449 lightning density over the plateau region. The color of the dots represents the CG
450 lightning density.

451

452 The aerosol loading over the basin region is much higher than that over the plateau
453 region, with sulfate AODs ranging from 0.2 to 0.9 (Fig. 10). Excessive aerosol loading
454 inhibits convective development through ARI. Aerosols reduce the solar radiation
455 reaching the surface through absorption and scattering, reducing the convective energy
456 of the surface and the lower atmosphere (Zhao et al., 2006; Jiang et al., 2018). Thus,
457 weak updrafts cannot transport liquid water above the freezing level. This may be why
458 the increase in aerosols leads to an increase in liquid water content and a decrease in
459 ice water content. Aerosols reduce the intensity of lightning activity by inhibiting the
460 development of convection and the formation of ice particles. This has also been
461 observed in other regions (Yang et al., 2013; Tan et al., 2016). CAPE is higher over the
462 basin region than over the plateau region (bottom panels of Fig. 11). An increase in
463 CAPE leads to a decrease in SHEAR and an increase in ice water content, promoting
464 the development of lightning, similar to the plateau region. Fan et al. (2009) found that
465 under large vertical wind shear conditions, an increase in aerosols inhibits the
466 development of convection. However, when CAPE exceeded 300 J kg^{-1} , an increase in
467 CAPE lead to a decrease in liquid water content. Convective clouds over the basin are



468 thicker than those over the plateau, and the high CAPE makes convection develop more
 469 vigorously. In this way, liquid water is transported above the freezing level to participate
 470 in the ice-phase process, forming more ice particles.



471
 472 **Figure 10.** Same as in Fig. 9, but for the basin region.

473
 474 According to the above, we hypothesize that the microphysical effect of aerosols
 475 is responsible for stimulating lightning activity over the plateau region and that the
 476 radiative effect of aerosols is responsible for suppressing lightning activity over the
 477 basin region. The radiative effect of aerosols impacts lightning by affecting CAPE,
 478 while the microphysical effect of aerosols impacts lightning by affecting the liquid
 479 water and ice water contents. To further verify the radiative effect of aerosols in the
 480 basin and the microphysical effect of aerosols in the plateau, two lightning sensitivity
 481 parameters are employed:

$$482 \quad RL_r = FC/CAPE, \quad (4)$$

483 where RL_r is a relative measure of lightning sensitivity to the effect of CAPE, associated
 484 with the aerosol radiative effect, and FC is the CG lightning flash count. Tinmaker et
 485 al. (2019) evaluated the impact of CAPE on lightning over land and oceanic regions by
 486 using $FC/CAPE$:

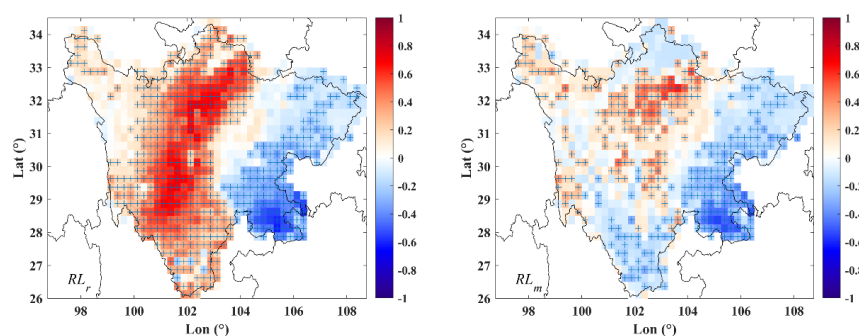
$$487 \quad RL_m = FC/(CAPE \times TCLW \times TCIW), \quad (5)$$

488 where RL_m is a relative lightning parameter accounting for the effect of TCLW and



489 TCIW on lightning, associated with the aerosol microphysical effect. Since CAPE is an
490 essential factor for generating lightning, it is also considered in this formulation.

491 Figure 11 shows the Pearson correlation coefficients between RL_r , RL_m , and sulfate
492 AOD over Sichuan. Compared with the correlation between sulfate AOD and CG
493 lightning (right panel of Fig. 3), the negative correlation between sulfate AOD and RL_r
494 decreased significantly in the basin area, especially in the northern part of the basin,
495 while the positive correlation between AOD and RL_r did not change significantly in the
496 plateau region. This suggests that the inhibitory effect of aerosols on lightning in the
497 basin region is dependent on the effect on CAPE, but not in the plateau region, which
498 also reflects the significant radiative effect of aerosols in the basin region. By
499 comparing the correlation between sulfate AOD and RL_m (right panel of Fig. 11) and
500 the correlation between sulfate AOD and CG lightning (right panel of Fig. 3), the
501 positive correlation coefficients between sulfate AOD and RL_m in the plateau region
502 decreased significantly, indicating that aerosols in the plateau region have a significant
503 microphysical effect, stimulating the development of lightning activity by influencing
504 liquid- and ice-phase particles in thunderstorms.



505 **Figure 11.** Same as in Fig. 3, but for RL_r (left panel) and RL_m (right panel).
506

507 3.5 Multiple linear regression of CG lightning

508 Because the physical processes involved in the development of lightning are
509 complex, many previous studies (e.g., Allen and Pickering, 2002; Tippett and Koshak,
510 2018) have parameterized lightning in weather and climate models by statistical



511 regression methods instead of describing the specific physical processes of lightning in
512 the model. Stolz et al. (2017) developed a global lightning parameterization scheme
513 based on multiple linear regression, combining aerosol and thermodynamic parameters,
514 which explained 69–81% of lightning activities in tropical and subtropical regions. The
515 multiple linear regression equations are based on the least-squares method and monthly
516 regionally averaged data. Since there is little or no lightning activity in winter, January,
517 February, and December are excluded. For the plateau region,

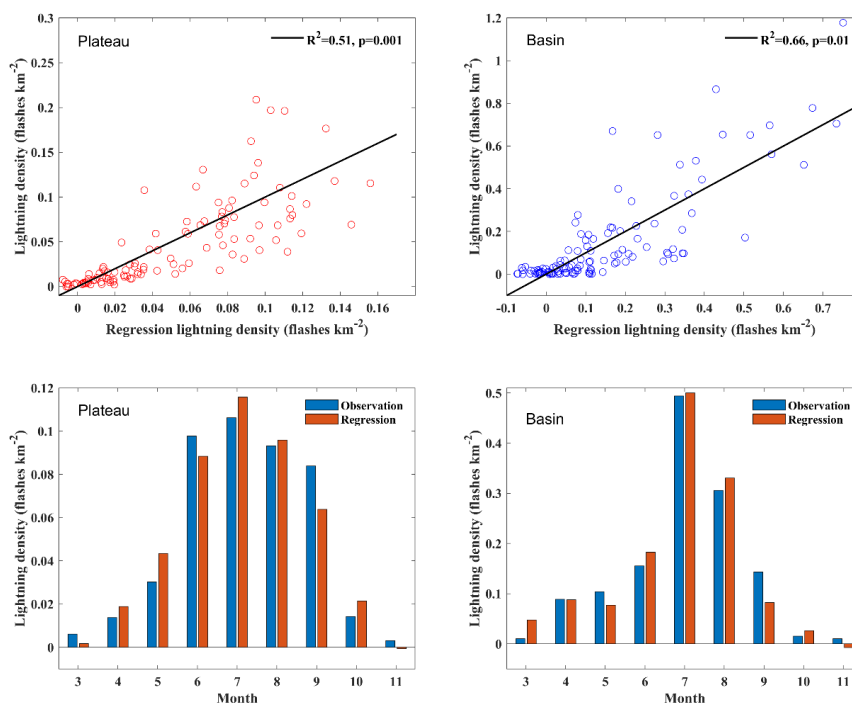
$$518 \quad Y = -0.023 + 0.52 \times 10^{-3}x_1 + 0.12 \times 10^{-3}x_2 - 6.01 \times 10^{-7}x_3 - 2.13 \times \\ 519 \quad 10^{-5}x_4 - 0.62x_5 - 0.14x_6 + 0.06x_7, \quad (6)$$

520 and for the basin region,

$$521 \quad Y = -0.29 + 0.49 \times 10^{-3}x_1 - 0.25 \times 10^{-2}x_2 - 0.77 \times 10^{-2}x_3 - 1.53 \times 10^{-5}x_4 + \\ 522 \quad 10.13x_5 + 0.19x_6 + 0.54x_7, \quad (7)$$

523 where Y is the CG lightning density, x_1 is CAPE, x_2 is RH, x_3 is SHEAR, x_4 is CBH, x_5
524 is TCIW, x_6 is TCLW, and x_7 is sulfate AOD.

525 Figure 12 shows scatter plots and monthly distributions of CG lightning densities
526 from multiple linear regression and observations in the plateau and basin regions. The
527 scatter plots show that the modeled lightning density tends to be lower than the
528 observed lightning density. The correlation in the basin region ($R^2 = 0.66$) is higher than
529 that in the plateau region ($R^2 = 0.51$), but both are lower than the correlation reported
530 by Stolz et al. (2017). Note that Stolz et al. (2017) examined total lightning on a global
531 scale while this study focuses on CG lightning formed over a region with complex
532 terrain. The monthly distributions of observed and modeled CG lightning densities in
533 the plateau and basin regions show that multiple linear regression can reproduce the
534 seasonal variations in lightning activity well. Overall, the best agreement in both
535 regions is seen in summer. The best agreements in the plateau and basin regions are
536 seen in August and July, respectively.



537 **Figure 12.** Scatter plots of observed CG lightning densities as a function of lightning
 538 densities from multiple linear regression in the plateau and basin regions (top panels)
 539 and their monthly distributions (bottom panels).

540

541 To further discuss the main impact factors that contribute to lightning, we use the
 542 stepwise regression method to select the top three impact factors. The stepwise
 543 regression equations based on the top three impact factors are as follows:

544 for the plateau region,

$$545 \quad Y = -0.011 + 0.52 \times 10^{-3}x_1 + 0.25 \times 10^{-3}x_2 - 9.41 \times 10^{-6}x_4, \quad (8)$$

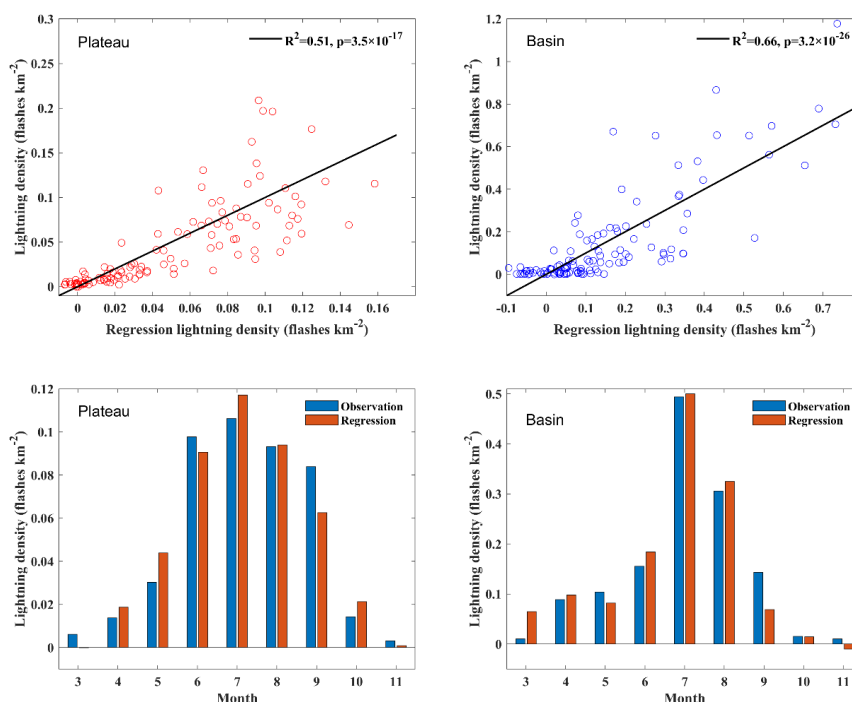
546 and for the basin region,

$$547 \quad Y = -0.48 + 0.55 \times 10^{-3}x_1 + 9.35x_5 + 0.53x_7, \quad (9)$$

548 where Y is the CG lightning density, x_1 is CAPE, x_2 is RH, x_4 is CBH, x_5 is TCIW, and
 549 x_7 is sulfate AOD. The top three factors contributing to lightning in the plateau region
 550 are CAPE, RH, and CBH, and the top three factors contributing to lightning in the basin
 551 region are CAPE, TCIW, and AOD, suggesting that aerosols have a more prominent
 552 effect on lightning in the basin region.



553 Figure 13 shows scatter plots and monthly distributions of CG lightning densities
554 from stepwise regression and observations in the plateau and basin regions. As seen in
555 Fig. 12, the modeled lightning density tends to be lower than the observed lightning
556 density, with R^2 values of 0.51 and 0.66 in the plateau and basin regions, respectively.
557 This also suggests that lightning activity can be reasonably modeled as long as factors
558 that contribute significantly to lightning, such as CAPE, are properly determined. The
559 monthly distributions of lightning densities modeled by stepwise regression agree with
560 observations from March to October reasonably well.



561 **Figure 13.** Scatter plots of observed CG lightning densities as a function of lightning
562 densities from stepwise regression in the plateau and basin regions (top panels) and
563 their monthly distributions (bottom panels).

564

565 4 Conclusions

566

567 In this study, we investigated the influence of aerosol, thermodynamic, and cloud-
568 related factors on CG lightning activity in the plateau and basin regions of Sichuan



569 province, a part of China with complex terrain. Data used to discuss the dependence of
570 the effect of aerosols on CG lightning on thermodynamic and cloud-related conditions
571 included the CG lightning density, sulfate AOD, CAPE, RH, SHEAR, CBH, TCLW,
572 and TCIW from 2005–2017.

573 CG lightning activity over the basin region was much more vigorous than that over
574 the plateau region, related to the thermodynamic difference between the two regions.
575 AODs in the basin region were also significantly higher than those in the plateau region,
576 mainly due to the large amounts of anthropogenic air pollutant emissions and the
577 mountainous terrain around the basin area that is not conducive to the diffusion of air
578 pollutants. CG lightning activity was positively correlated with AOD in the plateau
579 region, but negatively correlated with AOD in the basin region. The correlation between
580 sulfate AOD and lightning was stronger than that between total AOD and lightning, and
581 since sulfate AOD accounted for a high proportion of the total AOD, this study focused
582 on the role of sulfate AOD. The lightning density over the plateau region increased
583 exponentially with increasing AOD, while the lightning density over the basin region
584 decreased exponentially with increasing AOD.

585 CAPE, RH, and TCIW were significantly positively correlated with lightning
586 activity, while SHEAR was negatively correlated with lightning, suggesting that
587 convective uplift and ice-phase particles are essential factors for lightning activity. CBH
588 indirectly represents the warm-cloud thickness and is negatively correlated with TCLW.
589 The increase in TCLW in the plateau region is beneficial to lightning activity, but not
590 in the basin region, which may be related to the difference in warm-cloud depths
591 between the two regions. In the plateau region, because of the compression effect of the
592 plateau topography on clouds, warm clouds are very thin, and the high liquid water
593 content is conducive to conveying more supercooled water to the freezing level,
594 promoting the development of ice-phase clouds and lightning activity. In the basin
595 region, higher liquid water contents mean robust warm-cloud processes, which are more
596 conducive to the formation of warm rain than ice-phase processes, thus inhibiting
597 lightning activity. Partial correlation analyses indicate that CAPE, SHEAR, and TCIW



598 are important factors controlling lightning activity, especially CAPE.

599 To reveal the joint effects of aerosol, thermodynamic, and cloud-related factors on
600 CG lightning, AOD, CAPE, SHEAR, TCLW, TCIW were selected for further analysis.
601 In the plateau region, the aerosol loading is relatively low, stimulating lightning activity
602 through the microphysical effect. An increase in aerosol loading reduces the size of
603 cloud droplets, generating more but smaller cloud droplets, thus reducing the collision-
604 coalescence efficiency and inhibiting the warm-rain process. An increase in the liquid
605 water content of a cloud is conducive to the development of the ice-phase process,
606 which releases more latent heat and further stimulates convection. The increased
607 convection and the increase in ice particles lead to more intense lightning activity. In
608 the basin region, the aerosol loading is very high, which inhibits lightning activity
609 through the radiative effect. High concentrations of aerosols reduce the solar radiation
610 reaching the surface through absorption and scattering and reduce the convective
611 energy from the ground to the lower atmosphere. The weakening of the convective
612 uplift is not conducive to the transportation of liquid water above the freezing level and
613 inhibits the development of the ice-phase process. The weakening of convection and
614 the ice-phase process thus inhibits the intensity of lightning activity. The correlation
615 between RL_m and AOD and the correlation between RL_r and AOD further the idea that
616 aerosols over the plateau region affect the hydrometeor content in the atmosphere
617 through the microphysical effect, while aerosols over the basin region mainly affect
618 convective energy through the radiative effect, both of which affect lightning activity
619 differently.

620

621 *Data availability.* The CG lightning data can be obtained by contacting the first author
622 (zpg@cuit.edu.cn). MERRA-2 aerosol data can be download from
623 <https://disc.sci.gsfc.nasa.gov/MERRA/> (last access: 9 September 2019), and the ERA5
624 data are from <https://cds.climate.copernicus.eu/> (last access: 9 September 2019).

625

626 *Author contributions.* PZ and ZL designed the research ideas for this study; PZ carried



627 it out and prepared the manuscript; HX, Y. Zheng, FW, XJ, and Y. Zhou provided the
628 analysis ideas of meteorological and cloud-related parameters. MC edited the
629 manuscript.

630

631 *Competing interests.* The authors declare that they have no conflict of interest.

632

633 *Acknowledgments.* This research was jointly supported by the National Natural Science
634 Foundation of China (41905126, 41875169, 41705120), the National Key Research and
635 Development Project (2018YFC1505702), and the Key Laboratory for Cloud Physics
636 of China Meteorological Administration LCP/CMA (2017Z016). Pengguo Zhao
637 acknowledges China Scholarship Council for support (201808515075).

638

639 **References**

640 Allen, D. J., and Pickering, K. E.: Evaluating lightning flash rate parameterizations for
641 use in a global chemical transport model, *J. Geophys. Res. Atmos.*, 107(D23), 4711,
642 <https://doi.org/10.1029/2002JD002066>, 2002.

643 Altaratz, O., Koren, I., Yair, Y., and Price, C.: Lightning response to smoke from
644 Amazonian fires, *Geophys. Res. Lett.*, 37, L07801,
645 <https://doi.org/10.1029/2010GL042679>, 2010.

646 Altaratz, O., Kucienska, B., Kostinski, A., Raga, G. B., and Koren, I.: Global
647 association of aerosol with flash density of intense lightning, *Environ. Res. Lett.*,
648 12, 114037, <https://doi.org/10.1088/1748-9326/aa922b>, 2017.

649 Bang, S. D., and Zipser E. J.: Seeking reasons for the differences in size spectra of
650 electrified storms over land and ocean, *J. Geophys. Res. Atmos.*, 121, 9048–9068,
651 <https://doi.org/10.1002/2016JD025150>, 2016.

652 Buchard, V., Randles, C.A., Da Silva, A.M., Darmenov, A., Colarco, P.R., Govindaraju,
653 R., Ferrare, R., Hair, J., Beyersdorf, A.J., Ziemba, L.D. and Yu, H.: The MERRA-2
654 aerosol reanalysis, 1980 onward. Part II: Evaluation and case studies, *J. Climate*,
655 30(17), 6851–6872, <https://doi.org/10.1175/JCLI-D-16-0613.1>, 2017.



- 656 Carey, L. D., and Buffalo, K. M.: Environmental control of cloud-to-ground lightning
657 polarity in severe storms, *Mon. weather rev.*, 135(4), 1327–1353,
658 <https://doi.org/10.1175/MWR3361.1>, 2007.
- 659 Carrió, G. G., and Cotton, W. R.: On the buffering of CCN impacts on wintertime
660 orographic clouds: An idealized examination, *Atmos. Res.*, 137, 136–144,
661 <https://doi.org/10.1016/j.atmosres.2013.09.011>, 2014.
- 662 China Meteorological Administration, 2009: China Lightning Monitoring Reports (in
663 Chinese). China Meteorological Press, 142 pp., 2008.
- 664 Cummins, K. L., and Murphy, M. J., Bardo, E. A., Hiscox, W. L., Pyle, R. B., and Pifer,
665 A. E.: A combined TOA/MDF technology upgrade of the U.S. National Lightning
666 Detection Network, *J. Geophys. Res. Atmos.*, 103, 9035–9044,
667 <https://doi.org/10.1029/98JD00153>, 1998.
- 668 Cummins, K. L., and M. J. Murphy: An overview of lightning locating systems: History,
669 techniques, and data uses, with an in-depth look at the U.S. NLDN. *IEEE Trans.*
670 *Electromagn. Compat.*, 51, 499–518, <https://doi.org/10.1109/TEMC.2009.2023450>,
671 2009.
- 672 Dafis, S., Fierro, A., Giannaros, T. M., Kotroni, V., Lagouvardos, K. and Mansell, E.,
673 Performance evaluation of an explicit lightning forecasting system. *J. Geophys. Res.*
674 *Atmos.*, 123(10), 5130–5148, <https://doi.org/10.1029/2017JD027930>, 2018.
- 675 Dee, D. P., and Coauthors: The ERA-Interim reanalysis: Configuration and
676 performance of the data assimilation system. *Q. J. R. Meteorolog. Soc.*, 137(656),
677 553–597, <https://doi.org/10.1002/qj.828>, 2011.
- 678 Davies-Jones, R.: Linear and nonlinear propagation of supercell storms, *J. Atmos. Sci.*,
679 59, 3178–3205,
680 [https://doi.org/10.1175/15200469\(2003\)059<3178:LANPOS>2.0.CO;2](https://doi.org/10.1175/15200469(2003)059<3178:LANPOS>2.0.CO;2), 2002.
- 681 Fan, J., Yuan, T., Comstock, J. M., Ghan, S., Khain, A., Leung, L. R., Li, Z., Martins,
682 V. J. and Ovchinnikov, M.: Dominant role by vertical wind shear in regulating
683 aerosol effects on deep convective clouds. *J. Geophys. Res. Atmos.*, 114(D22),
684 <https://doi.org/10.1029/2009JD012352>, 2009.



- 685 Fan, J., Rosenfeld, D., Yang, Y., Zhao, C., Leung, L. R. and Li, Z.: Substantial
686 contribution of anthropogenic air pollution to catastrophic floods in Southwest
687 China. *Geophys. Res. Lett.*, 42(14), 6066–6075,
688 <https://doi.org/10.1002/2015GL064479>, 2015.
- 689 Fan, J., Rosenfeld, D., Zhang, Y., Giangrande, S., Li, Z., Machado, L., et al. Substantial
690 convection and precipitation enhancements by ultrafine aerosol particles. *Science*,
691 359(6374), 411–418. <https://doi.org/10.1126/science.aan8461>, 2018.
- 692 Freychet, N., Tett, S. F. B., Yan, Z., and Li, Z.: Underestimated change of wet-bulb
693 temperatures over East and South China, *Geophys. Res. Lett.*, 47, e2019GL086140,
694 <https://doi.org/10.1029/2019GL086140>, 2020.
- 695 Fuchs, B. R., Rutledge, S. A., Bruning, E. C., Pierce, J. R., Kodros, J. K., Lang, T. J.,
696 MacGorman, D. R., Krehbiel, P. R., and Rison, W.: Environmental controls on
697 storm intensity and charge structure in multiple regions of the continental United
698 States, *J. Geophys. Res. Atmos.*, 120, 6575–6596,
699 <https://doi.org/10.1002/2015JD023271>, 2015.
- 700 Guo, J., Deng, M., Lee, S.S., Wang, F., Li, Z., Zhai, P., Liu, H., Lv, W., Yao, W. and Li,
701 X.: Delaying precipitation and lightning by air pollution over the Pearl River Delta.
702 Part I: Observational analyses, *J. Geophys. Res. Atmos.*, 121, 6472–6488,
703 <https://doi.org/10.1002/2015JD023257>, 2016.
- 704 Hoffmann, L., Günther, G., Li, D., Stein, O., Wu, X., Griessbach, S., Heng, Y., Konopka,
705 P., Müller, R., Vogel, B. and Wright, J. S.: From ERA-Interim to ERA5: the
706 considerable impact of ECMWF’s next-generation reanalysis on Lagrangian
707 transport simulations, *Atmos. Chem. Phys.*, 19, 3097–3124,
708 <https://doi.org/10.5194/acp-19-3097-2019>, 2019.
- 709 Huang, J., Zhang, C., and Prospero, J. M.: Large-scale effect of aerosols on precipitation
710 in the West African Monsoon region, *Q. J. R. Meteorolog. Soc.*, 135 581–94,
711 <https://doi.org/10.1002/qj.391>, 2009.
- 712 Jiang, J. H., Su, H., Huang, L., Wang, Y., Massie, S., Zhao, B., Omar A, Wang, Z.:
713 Contrasting effects on deep convective clouds by different types of aerosols. *Nat.*



- 714 commun., 9(1), 1–7, <https://doi.org/10.1038/s41467-018-06280-4>, 2018.
- 715 Kar, S. K., Liou, Y. A., and Ha, K. J.: Aerosol effects on the enhancement of cloud-to-
716 ground lightning over major urban areas of South Korea, *Atmos. Res.*, 92, 80–87,
717 <https://doi.org/10.1016/j.atmosres.2008.09.004>, 2009.
- 718 Kar, S. K., and Liou, Y. A.: Enhancement of cloud-to-ground lightning activity over
719 Taipei, Taiwan in relation to urbanization, *Atmos. Res.*, 147–148, 111–120,
720 <https://doi.org/10.1016/j.atmosres.2014.05.017>, 2014.
- 721 Khain, A., Cohen, N., Lynn, B., Pokrovsky, A.: Possible aerosol effects on lightning
722 activity and structure of hurricanes, *J. Atmos. Sci.*, 65, 3652–3667,
723 <https://doi.org/10.1175/2008JAS2678.1>, 2008.
- 724 Koren, I., Martins, J. V., Remer, L. A. and Afargan, H.: Smoke invigoration versus
725 inhibition of clouds over the Amazon, *Science*, 321, 946–949,
726 <https://doi.org/10.1126/science.1159185>, 2008.
- 727 Koren, I., Altaratz, O., Remer, L. A., Feingold, G., Martins, J. V., and Heiblum, R. H.:
728 Aerosol-induced intensification of rain from the tropics to the mid-latitudes, *Nat.*
729 *Geosci.*, 5, 118–122, <https://doi.org/10.1038/ngeo1364>, 2012.
- 730 Koren, I., Dagan, G., and Altaratz, O.: From aerosol-limited to invigoration of warm
731 convective clouds, *Science*, 344, 1143–1146,
732 <https://doi.org/10.1126/science.1252595>, 2014.
- 733 Lee, S. S., Guo, J., and Li, Z.: Delaying precipitation by air pollution over the Pearl
734 River Delta: 2. Model simulations, *J. Geophys. Res. Atmos.*, 121, 11739–11760,
735 doi:10.1002/2015JD024362, 2016.
- 736 Lee, S., Hwang, S. O., Kim, J. and Ahn, M. H.: Characteristics of cloud occurrence
737 using ceilometer measurements and its relationship to precipitation over Seoul,
738 *Atmos. Res.*, 201, 46–57, <https://doi.org/10.1016/j.atmosres.2017.10.010>, 2018.
- 739 Lei, Y., Letu, H., Shang, H., and Shi, J.: Cloud cover over the Tibetan Plateau and
740 eastern China: a comparison of ERA5 and ERA-Interim with satellite observations,
741 *Clim. Dynam.*, 1–17, <https://doi.org/10.1007/s00382-020-05149-x>, 2020.
- 742 Li, Z., Niu, F., Fan, J., Liu, Y., Rosenfeld, D. and Ding, Y.: Long-term impacts of



743 aerosols on the vertical development of clouds and precipitation, *Nat. Geosci.*, 4(12),
744 888-894, <https://doi.org/10.1038/ngeo1313>, 2011.

745 Li, Z., Rosenfeld, D., Fan, J.: Aerosols and their impact on radiation, clouds,
746 precipitation, and severe weather events, *Oxford Research Encyclopedias*, PNNL-
747 SA-124900, <https://doi.org/10.1093/acrefore/9780199389414.013.126>, 2017.

748 Li, Z., Wang, Y., Guo, J., Zhao, C., Cribb, M. C., Dong, X., Fan, J., Gong, D., Huang,
749 J., Jiang, M. and Jiang, Y., et al.: East Asian Study of Tropospheric Aerosols and
750 their Impact on Regional Clouds, Precipitation, and Climate (EAST-AIR_{CPC}), *J.*
751 *Geophys. Res. Atmos.*, 124. <https://doi.org/10.1029/2019JD030758>, 2019, 2019.

752 Li, X., Pan, Y., and Mo, Z.: Joint effects of several factors on cloud-to-ground lightning
753 and rainfall in Nanning (China), *Atmos. Res.*, 212, 23–32,
754 <https://doi.org/10.1016/j.atmosres.2018.05.002>, 2018.

755 Lyons, W. A., Nelson, T. E., Williams, E. R., Cramer, J. A., and Turner, T. R.: Enhanced
756 positive cloud-to-ground lightning in thunderstorms ingesting smoke from fires,
757 *Science*, 282(5386), 77–80, <https://doi.org/10.1126/science.282.5386.77>, 1998.

758 MacGorman, D. R., Straka, J. M., Ziegler, C. L.: A lightning parameterization for
759 numerical cloud models, *J. Appl. Meteorol.*, 40, 459–478,
760 [https://doi.org/10.1175/1520-0450\(2001\)040<0459:ALPFNC>2.0.CO;2](https://doi.org/10.1175/1520-0450(2001)040<0459:ALPFNC>2.0.CO;2), 2001.

761 Mansell, E. R., MacGorman, D. R., Ziegler, C. L., Straka, J. M.: Charge structure and
762 lightning sensitivity in a simulated multicell thunderstorm, *J. Geophys. Res. Atmos.*,
763 110(D12): 1545–1555, <https://doi.org/10.1029/2004JD005287>, 2005.

764 Mansell, E. R., Ziegler, C. L.: Aerosol Effects on Simulated Storm Electrification and
765 Precipitation in a Two-Moment Bulk Microphysics Model, *J. Atmos. Sci.*, 70,
766 2032–2050, <https://doi.org/10.1175/JAS-D-12-0264.1>, 2013.

767 Minzner, R. A.: The 1976 standard atmosphere and its relationship to earlier standards.
768 *Rev. geophys.*, 15(3), 375-384, <https://doi.org/10.1029/RG015i003p00375>, 1977.

769 Naccarato, K. P., Pinto Jr, O., and Pinto, I. R. C. A.: Evidence of thermal and aerosol
770 effects on the cloud-to-ground lightning density and polarity over large urban areas
771 of Southeastern Brazil, *Geophys. Res. Lett.*, 30(13),



- 772 <https://doi.org/10.1029/2003GL017496>, 2003.
- 773 Ning, G., Wang, S., Yim, S., Li, J., Hu, Y., Shang, Z., Wang, J. and Wang, J.: Impact of
774 low-pressure systems on winter heavy air pollution in the northwest Sichuan Basin,
775 China, *Atmos. Chem. Phys.*, 18(18), 13601–13615, [https://doi.org/10.5194/acp-18-](https://doi.org/10.5194/acp-18-13601-2018)
776 13601-2018, 2018.
- 777 Oreopoulos, L., Cho, N., and Lee, D.: A global survey of apparent aerosol-cloud
778 interaction signals, *J. Geophys. Res.*, 125, e2019JD031287,
779 <https://doi.org/10.1029/2019JD031287>, 2020.
- 780 Orville, R. E., Huffines, G. R., Burrows, W. R., and Cummins, K. L.: The North
781 American lightning detection network (NALDN)-Analysis of flash data: 2001–09,
782 *Mon. Weather Rev.*, 139(5), 1305–1322, <https://doi.org/10.1175/2010MWR3452.1>,
783 2011.
- 784 Pawar, S. D., Gopalakrishnan, V., Murugavel, P., Veremey, N. E. and Sinkevich, A. A.:
785 Possible role of aerosols in the charge structure of isolated thunderstorms. *Atmos.*
786 *Res.*, 183, 331–340, <https://doi.org/10.1016/j.atmosres.2016.09.016>, 2017.
- 787 Pinto, I. R. C. A., Pinto, Jr O., Gomes, M. A. S. S., Ferreira, N. J.: Urban effect on the
788 characteristics of cloud-to-ground lightning over Belo Horizonte-Brazil, *Ann.*
789 *Geophys.*, 22, 697–700, 2004.
- 790 Price, C. G.: Lightning Applications in Weather and Climate Research, *Surv. Geophys.*,
791 34, 755–767. <https://doi.org/10.1007/s10712-012-9218-7>, 2013.
- 792 Proestakis, E., Kazadzis, S., Lagouvardos, K., Kotroni, V., and Kazantzidis, A.:
793 Lightning activity and aerosols in the Mediterranean region, *Atmos. Res.*, 170, 66–
794 75, <https://doi.org/10.1016/j.atmosres.2015.11.010>, 2016.
- 795 Qian, Y., Gong, D., Fan, J., Leung, L. R., Bennartz, R., Chen, D., and Wang, W.: Heavy
796 pollution suppresses light rain in China: Observations and modeling. *J. Geophys.*
797 *Res. Atmos.*, 114(D7), <https://doi.org/10.1029/2008JD011575>, 2009.
- 798 Qie, X., and Zhang, Y.: A Review of Atmospheric Electricity Research in China from
799 2011 to 2018, *Adv. Atmos. Sci.*, 36, 994–1014, [https://doi.org/10.1007/s00376-019-](https://doi.org/10.1007/s00376-019-8195-x)
800 8195-x, 2019.



- 801 Ramos, A. M., R. Ramos, P. Sousa, R. M. Trigo, M. Janeira, and Prior, V.: Cloud to
802 ground lightning activity over Portugal and its association with circulation weather
803 types, *Atmos. Res.*, 101, 84–101, <https://doi.org/10.1016/j.atmosres.2011.01.014>,
804 2011.
- 805 Randles, C. A., Da Silva, A. M., Buchard, V., Colarco, P. R., Darmenov, A., Govindaraju,
806 R., Smirnov, A., Holben, B., Ferrare, R., Hair, J. and Shinozuka, Y.: The MERRA-
807 2 aerosol reanalysis, 1980 onward. Part I: System description and data assimilation
808 evaluation. *J. Climate*, 30(17), 6823–6850, <https://doi.org/10.1175/JCLI-D-16-0609.1>, 2017.
- 810 Romps, D. M., Seeley, J. T., Vollaro, D. and Molinari, J.: Projected increase in lightning
811 strikes in the United States due to global warming, *Science*, 346(6211), 851–854,
812 <https://doi.org/10.1126/science.1259100>, 2014.
- 813 Romps, D. M., Charn, A. B., Holzworth, R. H., Lawrence, W. E., Molinari, J., and
814 Vollaro, D.: CAPE times P explains lightning over land but not the land-ocean
815 contrast. *Geophys. Res. Lett.*, 45, 12, 623–12, 630,
816 <https://doi.org/10.1029/2018GL080267>, 2018.
- 817 Rosenfeld, D., Dai, J., Yu, X., Yao, Z., Xu, X., Yang, X., and Du, C.: Inverse relations
818 between amounts of air pollution and orographic precipitation, *Science*, 315: 1396–
819 1398, <https://doi.org/10.1126/science.1137949>, 2007.
- 820 Rosenfeld, D., Lohmann, U., Raga, G. B., O'Dowd, C. D., Kulmala, M., Fuzzi, S.,
821 Reissell, A. and Andreae, M. O.: Flood or Drought: How Do Aerosols Affect
822 Precipitation, *Science*, 321: 1309–1313, <https://doi.org/10.1126/science.1160606>,
823 2008.
- 824 Saunders, C.: Charge separation mechanisms in clouds, *Space Sci. Rev.*, 137, 335–53,
825 <https://doi.org/10.1007/s11214-008-9345-0>, 2008.
- 826 Saunders, C. P. R., Keith, W. D., and Mitzeva. R. P.: The effect of liquid water on
827 thunderstorm charging, *J. Geophys. Res. Atmos.*, 96, 11007–17,
828 <https://doi.org/10.1029/91JD00970>, 1991.
- 829 Shi, Z., Tan, Y., Tang, H., Sun, J., Yang, Y., Peng, L. and Guo, X.: Aerosol effect on the



830 land-ocean contrast in thunderstorm electrification and lightning frequency. *Atmos.*
831 *Res.*, 164-165: 131-141, <https://doi.org/10.1016/j.atmosres.2015.05.006>, 2015.

832 Shou, Y., Lu, F., Liu, H., Cui, P., Shou, S., and Liu, J.: Satellite-based observational
833 study of the Tibetan Plateau Vortex: Features of deep convective cloud tops, *Adv.*
834 *Atmos. Sci.*, 36(2), 189–205, <https://doi.org/10.1007/s00376-018-8049-y>, 2019.

835 Stallins, J. A., Carpenter, J., Bentley, M. L., Ashley, W. S. and Mulholland, J. A.:
836 Weekend-weekday aerosols and geographic variability in cloud-to-ground lightning
837 for the urban region of Atlanta, Georgia, USA. *Reg. Environ. Change*, 13(1), 137–
838 151, <https://doi.org/10.1007/s10113-012-0327-0>, 2013.

839 Stolz, D. C., Rutledge, S. A., and Pierce, J. R.: Simultaneous influences of
840 thermodynamics and aerosols on deep convection and lightning in the tropics, *J.*
841 *Geophys. Res. Atmos.*, 120(12), 6207–6231,
842 <https://doi.org/10.1002/2014JD023033>, 2015.

843 Stolz, D. C., Rutledge, S. A., Pierce, J. R., and van den Heever, S. C.: A global lightning
844 parameterization based on statistical relationships among environmental factors,
845 aerosols, and convective clouds in the TRMM climatology, *J. Geophys. Res. Atmos.*,
846 122, 7461-7492, <https://doi.org/10.1002/2016JD026220>, 2017.

847 Sun, E., Che, H., Xu, X., Wang, Z., Lu, C., Gui, K., Zhao, H., Zheng, Y., Wang, Y.,
848 Wang, H. and Sun, T.: Variation in MERRA-2 aerosol optical depth over the
849 Yangtze River Delta from 1980 to 2016, *Theor. Appl. Climatol.*, 136(1-2),
850 <https://doi.org/10.1007/s00704-018-2490-9>, 363-375, 2019a.

851 Sun, E., Xu, X., Che, H., Tang, Z., Gui, K., An, L., Lu, C., and Shi, G.: Variation in
852 MERRA-2 aerosol optical depth and absorption aerosol optical depth over China
853 from 1980 to 2017. *J. Atmos. Sol.-Terr. Phy.*, 186, 8-19,
854 <https://doi.org/10.1016/j.jastp.2019.01.019>, 2019b.

855 Sun, L., Wei, J., Duan, D. H., Guo, Y. M., Yang, D. X., Jia, C., and Mi, X.: Impact of
856 Land-Use and Land-Cover Change on urban air quality in representative cities of
857 China. *J. Atmos. Sol.-Terr. Phy.*, 142, 43-54,
858 <https://doi.org/10.1016/j.jastp.2016.02.022>, 2016.



- 859 Tan, Y., Peng, L., Shi, Z. and Chen, H.: Lightning flash density in relation to aerosol
860 over Nanjing (China), *Atmos. Res.*, 174, 1-8,
861 <https://doi.org/10.1016/j.atmosres.2016.01.009>, 2016.
- 862 Thompson, R. L., Mead, C. M., and Edwards, R.: Effective storm-relative helicity and
863 bulk shear in supercell thunderstorm environments, *Weather Forecast.*, 22, 102–115,
864 <https://doi.org/10.1175/WAF969.1>, 2007.
- 865 Thornton, J. A., Virts, K. S., Holzworth, R. H. and Mitchell, T. P.: Lightning
866 enhancement over major oceanic shipping lanes, *Geophys. Res. Lett.*, 44(17), 9102-
867 9111, <https://doi.org/10.1002/2017GL074982>, 2017.
- 868 Tinmaker, M. I. R., Ghude, S. D., Chate, D. M.: Land-sea contrasts for climatic
869 lightning activity over Indian region, *Theor. Appl. Climatol.*, 138(1-2), 931-940,
870 <https://doi.org/10.1007/s00704-019-02862-4>, 2019.
- 871 Tippett, M. K., and Koshak, W. J.: A baseline for the predictability of U.S. cloud-to-
872 ground lightning. *Geophys. Res. Lett.*, 45, 10719–10728,
873 <https://doi.org/10.1029/2018GL079750>, 2018.
- 874 Tippett, M. K., Lepore, C., Koshak, W. J., Chronis, T. and Vant-Hull, B.: Performance
875 of a simple reanalysis proxy for US cloud-to-ground lightning. *Int. J. Climatol.*,
876 39(10), 3932-3946, <https://doi.org/10.1002/joc.6049>, 2019.
- 877 Wall, C., Zipser, E. J., and Liu, C.: An investigation of the aerosol indirect effect on
878 convective intensity using satellite observations, *J. Atmos. Sci.*, 71, 430–447,
879 <https://doi.org/10.1175/JAS-D-13-0158.1>, 2014.
- 880 Wang, Y., Wan, Q., Meng, W., Liao, F., Tan, H., and Zhang, R.: Long-term impacts of
881 aerosols on precipitation and lightning over the Pearl River Delta megacity area in
882 China. *Atmos. Chem. Phys.*, 11, 12421–12436, <https://doi.org/10.5194/acp-11-12421-2011>, 2011.
- 884 Wang, Q., Li, Z., Guo, J., Zhao, C. and Cribb, M.: The climate impact of aerosols on
885 the lightning flash rate: is it detectable from long-term measurements?, *Atmos.*
886 *Chem. Phys.*, 18(17), 12797–12816, <https://doi.org/10.5194/acp-18-12797-2018>,
887 2018.



- 888 Wei, J., Huang, W., Li, Z., Xue, W., Peng, Y., Sun, L., and Cribb, M.: Estimating 1-km-
889 resolution PM_{2.5} concentrations across China using the space-time random forest
890 approach, *Remote Sens. Environ.*, 231, 111221,
891 <https://doi.org/10.1016/j.rse.2019.111221>, 2019a.
- 892 Wei, J., Li, Z., Guo, J., Sun, L., Huang, W., Xue, W., Fan, T., and Cribb, M. Satellite-
893 derived 1-km-resolution PM₁ concentrations from 2014 to 2018 across China,
894 *Environmen. Sci. Technol.*, 53(22), 13265–13274,
895 <https://doi.org/10.1021/acs.est.9b03258>, 2019b.
- 896 Westcott, N. E.: Summertime cloud-to-ground lightning activity around major
897 Midwestern urban areas, *J. Appl. Meteorol.*, 34: 1633-1642,
898 <https://doi.org/10.1175/1520-0450-34.7.1633>, 1995.
- 899 Williams, E. R.: Lightning and climate: A review. *Atmos. Res.*, 76, 272-287,
900 <https://doi.org/10.1016/j.atmosres.2004.11.014>, 2005.
- 901 Williams, E. and Stanfill, S.: The physical origin of the land-ocean contrast in lightning
902 activity. *C. R. Phys.*, 3(10), 1277-1292, [https://doi.org/10.1016/S1631-](https://doi.org/10.1016/S1631-0705(02)01407-X)
903 [0705\(02\)01407-X](https://doi.org/10.1016/S1631-0705(02)01407-X), 2002.
- 904 Williams, E. R., Chan, T., and Boccippio, D.: Islands as miniature continents: another
905 look at the land ocean lightning contrast, *J. Geophys. Res. Atmos.*, 109,
906 <https://doi.org/10.1029/2003JD003833>, 2004.
- 907 Williams, E. R., Mushtak, V., Rosenfeld, D., Goodman, S., and Boccippio, D.:
908 Thermodynamic conditions favorable to superlative thunderstorm updraft, mixed
909 phase microphysics and lightning flash rate, *Atmos. Res.*, 76, 288–306,
910 <https://doi.org/10.1016/j.atmosres.2004.11.009>, 2005.
- 911 Wong, J., Barth, M.C. and Noone, D.: Evaluating a lightning parameterization based on
912 cloud-top height for mesoscale numerical model simulations, *Geosci. Model Dev.*,
913 6(2), 429–443, <https://doi.org/10.5194/gmd-6-429-2013>, 2013.
- 914 Xia, R., Zhang, D. L., and Wang, B.: A 6-yr cloud-to-ground lightning climatology and
915 its relationship to rainfall over central and eastern China. *J. Appl. Meteorol. Clim.*,
916 54(12), 2443–2460, <https://doi.org/10.1175/JAMC-D-15-0029.1>, 2015.



- 917 Yair, Y., Lynn, B., Price, C., Kotroni, V., Lagouvardos, K., Morin, E., Mugnai, A. and
918 Llasat, M. D. C.: Predicting the potential for lightning activity in Mediterranean
919 storms based on the Weather Research and Forecasting (WRF) model dynamic and
920 microphysical fields. *J. Geophys. Res. Atmos.*, 115(D4),
921 <http://dx.doi.org/10.1029/2008JD010868>, 2010.
- 922 Yair, Y. Lightning hazards to human societies in a changing climate. *Environ. Res. Lett.*,
923 13(12), 123002, <http://dx.doi.org/10.1088/1748-9326/aaea86>, 2018.
- 924 Yang, X., Yao, Z., Li, Z. and Fan, T.: Heavy air pollution suppresses summer
925 thunderstorms in central China. *J. Atmos. Sol.-Terr. Phy.*, 95,
926 <https://doi.org/10.1016/j.jastp.2012.12.023>, 28–40, 2013.
- 927 Yang, X., and Li, Z.: Increases in thunderstorm activity and relationships with air
928 pollution in southeast China, *J. Geophys. Res. Atmos.*, 119, 1835–1844,
929 <https://doi.org/10.1002/2013JD021224>, 2014.
- 930 Yang, X., Li, Z., Liu, L., Zhou, L., Cribb, M., and Zhang, F.: Distinct weekly cycles of
931 thunderstorms and a potential connection with aerosol type in China, *Geophys. Res.*
932 *Lett.*, 43, 8760–8768, [10.1002/2016GL070375](https://doi.org/10.1002/2016GL070375), 2016.
- 933 Yang, X., Sun, J., and Li, W.: An analysis of cloud-to-ground lightning in China during
934 2010–13, *Weather Forecast.*, 30(6), 1537–1550, [https://doi.org/10.1175/WAF-D-](https://doi.org/10.1175/WAF-D-14-00132.1)
935 14-00132.1, 2015.
- 936 Yu, R., Xu, Y., Zhou, T., and Li, J.: Relation between rainfall duration and diurnal
937 variation in the warm season precipitation over central eastern China, *Geophys. Res.*
938 *Lett.*, 34, L13703, <https://doi.org/10.1029/2006GL028129>, 2007.
- 939 Yuan, T., Remer, L. A., Pickering, K. E., Yun, H.: Observational evidence of aerosol
940 enhancement of lightning activity and convective invigoration, *Geophys. Res. Lett.*,
941 38, L04701, <https://doi.org/10.1029/2010GL046052>, 2011.
- 942 Zhang, X., Wang, Y., Niu, T., Zhang, X., Gong, S., Zhang, Y., and Sun, J.: Atmospheric
943 aerosol compositions in China: spatial/temporal variability, chemical signature,
944 regional haze distribution and comparisons with global aerosols. *Atmos. Chem.*
945 *Phys.*, 12: 779–799, <https://doi.org/10.5194/acp-12-779-2012>, 2012.



- 946 Zhang, Y., Sun, J. and Fu, S.: Impacts of diurnal variation of mountain-plain solenoid
947 circulations on precipitation and vortices east of the Tibetan Plateau during the mei-
948 yu season, *Adv. Atmos. Sci.*, 31, 139–153, [https://doi.org/10.1007/s00376-013-](https://doi.org/10.1007/s00376-013-2052-0)
949 2052-0, 2014.
- 950 Zhang, Y., Cai, C., Chen, B. and Dai, W.: Consistency evaluation of precipitable water
951 vapor derived from ERA5, ERA-Interim, GNSS, and radiosondes over China.
952 *Radio Sci.*, 54(7), 561–571, <https://doi.org/10.1029/2018RS006789>, 2019.
- 953 Zhao, C., Tie, X. and Lin, Y.: A possible positive feedback of reduction of precipitation
954 and increase in aerosols over eastern central China, *Geophys. Res. Lett.*, 33, L11814,
955 <https://doi.org/10.1029/2006GL025959>, 2006.
- 956 Zhao, C., Lin, Y., Wu, F., Wang, Y., Li, Z., Rosenfeld, D., and Wang, Y.: Enlarging
957 rainfall area of tropical cyclones by atmospheric aerosols, *Geophys. Res. Lett.*, 45,
958 8604–8611, <https://doi.org/10.1029/2018GL079427>, 2018.
- 959 Zhao, P., Yin, Y. and Xiao, H.: The effects of aerosol on development of thunderstorm
960 electrification: A numerical study, *Atmos. Res.*, 153, 376–391,
961 <https://doi.org/10.1016/j.atmosres.2014.09.011>, 2015.